Inversion modeling optimization using CalCOFI data set

Young-Je Park*^a, Mati Kahru^b, and B. Greg Mitchell^b

^aEarth Observation Research Center, National Space Development Agency of Japan, Tokyo ^bScripps Institute of Oceanography, University of California, San Diego, La Jolla, California

ABSTRACT

A model of particle absorption coefficients is presented as a function of chlorophyll concentration. The model has been derived from remote sensing reflectance and chlorophyll concentration of CalCOFI bio-optical data set, using a radiance model. Variance in absorption coefficient for a given chlorophyll concentration can be reduced by introducing site-dependent particle backscattering coefficients, average of which is assumed to follow Morel's backscattering model. With an empirical algorithm for estimating the absorption by dissolved organic matter, we separate the absorption by particles from the total absorption. Through a simple quality control, statistical regression gives the parameterization of particle absorption. By applying the derived model to a semi-analytical inversion algorithm, we demonstrate the proposed model could be used to retrieve in-water parameters such as chlorophyll concentration, absorption by colored dissolved organic matter and particle backscattering coefficients.

Keywords: ocean color, inversion, absorption, backscattering, remote sensing, chlorophyll

1. INTRODUCTION

Many satellite-borne ocean-color sensors have been developed to provide the global or local distribution of pigment/chlorophyll concentration and finally to better assess the global carbon cycle. The operational routine algorithms for chlorophyll utilize the ratio of normalized water-leaving radiance (nLw) or remote-sensing reflectance (R_{rs}) at blue and green bands. The equations of the algorithms are derived by statistical analysis of in situ data sets of nLw (or R_{rs}) and chlorophyll a concentration (CHLA). These band ratio algorithms have been successful for case 1 waters, because the ratio of nLw at two bands can greatly reduce the effect of variabilities or uncertainties in each nLw data for a given CHLA. The variabilities include natural variability in backscattering coefficients, uncertainties in bidirectional reflectance and residual errors of atmospheric correction. Meanwhile, besides CHLA product, there have been scientific interests in other bio-optical properties including phytoplankton type, accessory pigments, colored dissolved organic matter (CDOM) and suspended sediment. The operational algorithms for these parameters are still under development or remain to be verified. Furthermore, in coastal case 2 waters, the global band-ratio algorithm is no more valid where the water reflectance can be controlled by the presence of other elements than phytoplankton. For example, current routine algorithms interpret a CDOM-rich water as case 1 water and give high pigment concentration. Some of the issues might be solved if semianalytical inversion algorithms will be successful. The inversion algorithms provide some inherent optical properties (IOPs) such as absorption and backscattering coefficients of constituents together with CHLA.²⁻⁴ The simultaneous retrieval of IOPs is desirable because, for example, the absorption by CDOM⁵ and scattering by particles⁶ are not well correlated with CHLA even in case 1 waters. Furthermore, since IOPs are directly related to in-water constituents, it is, in principle, more reasonable to retrieve in-water parameters from IOPs, which are estimated by inversion of the radiance model.

In general, an inversion algorithm consists of a radiance (reflectance) model, a set of IOP models and a technique to invert the radiance model. The radiance models have been well studied as far as subsurface reflectance is concerned, and widely used for analysis of ocean reflectance.⁷ There are several solution methods to invert the radiance models.²⁻⁴ On the other hand, IOPs such as chlorophyll specific absorption coefficient and backscattering coefficient show quite large uncertainty for a given CHLA over various oceanic waters. It is reported that absorption coefficient at 440 nm by phytoplankton exhibit a variability of several orders of magnitude.^{8,9} One of motivations of this study is to see if such large variability can be seen in absorption coefficients derived from data sets of R_{rs} and CHLA measured in a local area. Besides the model for absorption coefficients of phytoplankton, what else of IOPs are necessary for inversion algorithms? It depends on independent parameters to be retrieved. As described in following section, we will assume here three parameters of CHLA, CDOM, particle backscattering (for total suspended particles) to be independent in oceanic waters. Then we need the model

^{*}Correspondence: Email: park@eorc.nasda.go.jp; Telephone: +81-3-3224-7017

for absorption by phytoplankton and its associated particles as a function of CHLA and wavelength, and also the spectral behavior for each of CDOM absorption and particle backscattering. The last two properties are also significantly variable over different waters, which is out of the scope of this study. However to retrieve particle absorption from R_{rs} and CHLA data, we have to assume certain constants for these properties.

In this paper, we describe an approach to obtain the model for particle absorption from *in situ* measurements of CHLA and R_{rs} at several bands, with assuming the spectral shape of CDOM absorption and particle backscattering. We will show that the derived model works well with an inversion algorithm by retrieval of CHLA, CDOM and particle backscattering coefficients. Actually, a majority of bio-optical data set includes CHLA and R_{rs} that is derived from downward irradiance and upwelling radiance under water or above surface. The collected data set (eg. see Ref. 1) covers almost entire global ocean. Therefore, we believe that this approach will very useful in that it can utilize the existing large amount of *in situ* data.

2. THE RADIANCE AND IOP MODELS

In this section, we explain the radiance and IOP models that are necessary for retrieve the absorption coefficients from the data of R_{rs} and CHLA. The inherent optical properties (IOPs) are related to the apparent optical properties (AOPs) by the radiative transfer equation. For interpretation of remotely sensed data, several simplified models for radiance have been proposed and widely used. A radiance model here means an approximated analytical relationship between the IOPs and R_{rs} or nLw. These models can greatly reduce computing time compared to directly solving the radiative transfer equation. It has been derived by a number of numerical simulations of radiative transfer in various oceanic conditions^{7,10,11} or by analytical simplification. ¹² Both result in similar expressions.

One of issues in underwater radiative transfer simulations is how to simulate the change the backscattering probabilities of particle scattering with CHLA in case 1 waters, which is evident from analysis of in situ measurements. 13 Change of backscattering probability results from the change of the scattering phase functions which depend on the size distribution and refractive indices of suspended particles. It is expectable that small particle portion decreases as CHLA increases. However, as far as we know, all models mentioned above are generated without discerning the change of volume scattering function with trophic state. To our knowledge, there is no systematic study or measurements on the volume scattering functions in various oceanic conditions for radiance transfer study inside water. Therefore, we would approximate this systematic change with CHLA by linear combinations of two extreme-case phase functions, one of which is for large particles like phytoplankton and the other is for small particles like detritus. We used Kopelevich's volume scattering functions for these phase functions.¹⁴ The details of the two phase functions are described in Ref. 14. We change the proportion of the two phase functions so that the backscattering probability might follow Morel's estimation¹³ as a function of CHLA. Simulations were made using Hydrolight code¹⁵ with CHLA from 0.03 to 30 mg/m³ at wavelengths of 412, 443, 490, 520, 565 and 666 nm. For simplicity, we assume homogeneous medium. We did not include tran-spectral effects such as Raman scattering and chlorophyll/CDOM fluorescence in these simulations. These effects are negligible for radiance values in near surface, in which we have interest. Two extreme cases of input radiance distribution were used. One is the case of direct sun at zenith without sky and the other is Cardional distribution. (Note there are two points correspondent to one condition of IOP i.e., same value of Gordon parameter in the Figure 1) Both cases give very similar output as shown in the figure. For modeling under-water measurements of radiance and irradiance, we take the ratio of upwelling radiance to downwelling radiance, L_u/E_d , just below surface, denoted by r_{rs} in this paper. The computed values of subsurface r_{rs} were fitted to power functions of Gordon's parameter, b_b/(a+b_b). We choose power functions to fit with, because it minimizes relative errors rather than absolute errors. Since water contribution to total absorption and scattering is significantly changed in different wavelengths, we make regression independently for different bands, which can give better agreement with simulation results especially in longer waveband. The final model is expressed as follows:

$$\operatorname{rrs} = \frac{L_{u}(0^{-})}{E_{d}(0^{-})} = \alpha(\lambda) \left(\frac{b_{b}}{a + b_{b}}\right)^{\beta(\lambda)}, \tag{1}$$

where a and b_b are total absorption and backscattering coefficients at each wavelength, respectively and α and β are wavelength dependent constants. For simplicity, we do not show explicitly the wavelength dependence of parameters if not necessary. The values of α and β are tabulated in Table 1.

Table 1. The parameters of α and β in radiance model in Equation (1)

Center wavelength	412 nm	443 nm	490 nm	520 nm	565 nm	666 nm
α	0.1255	0.1282	0.1376	0.1002	0.0718	0.0593

106 Proc. SPIE Vol. 4154

Ī	β	1.082	1.092	1.114	1.010	0.917	0.927
	P	1.002	1.072	1.11.	1.010	0.717	0.727

The radiance model proposed here has good agreement with others^{7, 11} within about 5 % difference in most cases. In shorter wavebands (412, 443, and 490 nm), the difference is negligible (Figure 1(a)). But in longer wavebands (520, 565, and 666 nm), we can notice the difference (Figure 1(b)) even if it is much smaller than the realistic measurement error in these wavebands.

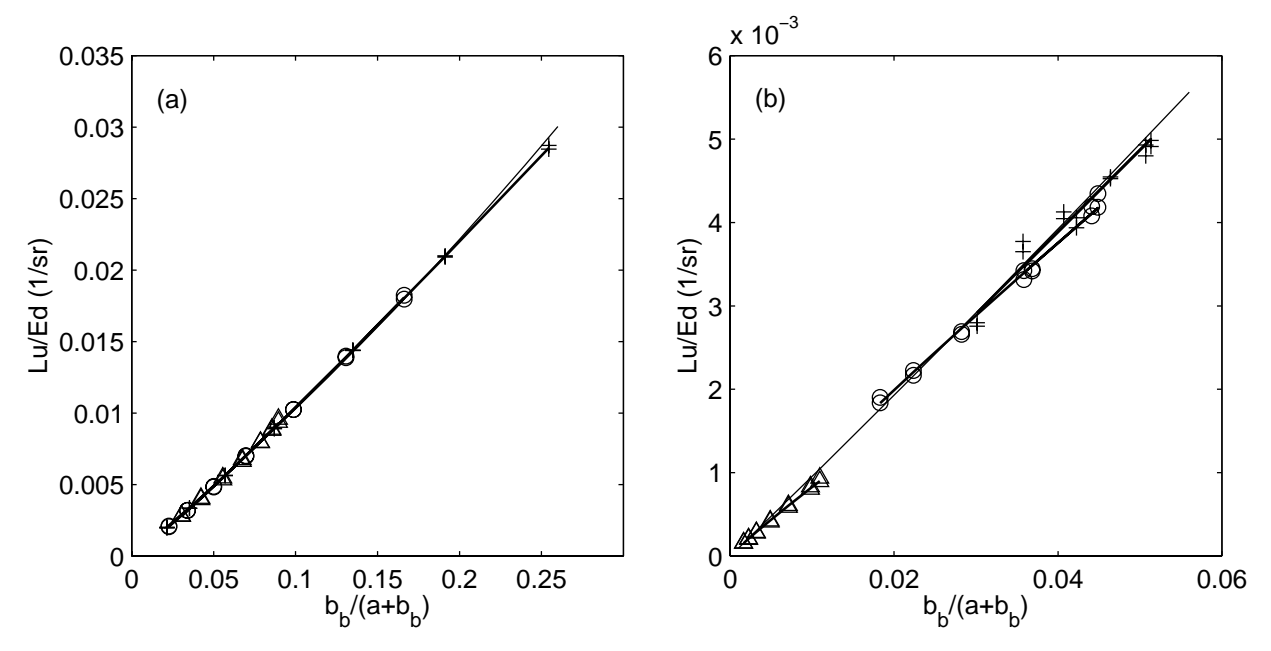


Figure 1. The ratios of subsurface upwelling radiance to downward irradiance plotted with Gordon's parameter; symbols of plus, circle and triangle denote for 412, 443, and 490 nm respectively in (a); for 520, 565, and 666nm, respectively in (b); thick lines for best fitted lines, Eq. (1) for each bands and thin lines represent Gordon's model.⁷

Total absorption of seawater is expressed as sum of the contributions of pure water (a_w) , particulate matter (a_p) and CDOM (a_g) . In oceanic waters, all suspended, light-absorbing particles are supposed to be related to bio-chemical process, and therefore they can be classified as two groups of phytoplankton and associated particles (mainly detrital particles). The absorption of detrital particles can be modeled independently with CHLA and it is combined with CDOM absorption, because the spectral behavior of CDOM absorption and detrital absorption is similar, though slope constants are different. In our analysis, for simplicity, we assume that detrital particles covary with CHLA. It does not make significant difference in final result, because detrital absorption is usually much smaller than chlorophyll absorption. Therefore we express the absorption by particles as a function of single parameter of CHLA, ignoring the uncertainties of the pigment composition and the portion of detritus. Absorption by CDOM exponentially decreases with wavelength. Therefore, the bio-optical dependence of the total absorption can be given as follows:

$$a = a_w(\lambda) + a_p(\lambda, CHLA) + a_q(440) \exp(-S(\lambda - 440)),$$
 (2)

where slope constant, S is variable depending on the composition of dissolved organics. We take the value of 0.0185 as S for our analysis. This value is average of measurements in California Current. Constant values of $a_w(\lambda)$ are taken from Pope and Fry. Similarly, total backscattering is the sum of contributions of pure water (b_{bw}) and particulate matter (b_{bp}) . Considering no strong correlation between backscattering by particles and CHLA even in oceanic waters, we do not relate the particle backscattering coefficient with CHLA for the data of individual station. Then the backscattering is expressed as:

$$b_b = b_{bw}(\lambda) + b_{bp}(550) \left(\frac{550}{\lambda}\right)^n,$$
 (3)

where n is variable from the size distribution of suspended particles. For this study, we assume constant value n (=1) is assumed for all data. Constant values of $b_w(\lambda)$ are taken from Smith and Baker. In summary, we set three independent parameters that determine IOP: CHLA, CDOM absorption at 440 nm and particle backscattering coefficients at 550 nm. In the following section, with estimation of last two parameters we get to particle absorption as a function of CHLA.

3. CALCOFI DATA SET AND MODELING PARTICLE ABSORPTION COEFFICIENTS

CalCOFI bio-optical data set is one of largest data sets currently available worldwide, and all the data are measured and quality-controlled in a consistent way. Detailed information on the data set can be found in Mitchell and Kahru. Although the area is limited in California current, the measured CHLA spans wide range (0.05 to 30 mg/m³), which is comparable to the globally measured range except low concentration. For this study, we used 459 sets of R_{rs} and CHLA data at commonly used ocean-color bands centered at 412, 443, 490, 520, 565, and 666 nm. The data of R_{rs} was obtained from subsurface data of upwelling radiance (L_u) and downward irradiance (E_d) that had been interpolated from underwater measurements. The relationship between R_{rs} and r_{rs} is described in Ref. 10. When there was no channel corresponding to a GLI band, the cubic spline interpolation was performed to get the R_{rs} at the GLI band center. Basically we may have errors due to interpolation as well as due to the difference in spectral response functions. However, we believe that these errors are much smaller than the variance in measured radiance for a given CHLA as shown in Figure 2. The variance of radiance can be from environmental condition as well as IOP variations. The environmental condition includes wind speed, solar elevation, sky radiance, and so on. IOP variation includes the variation in pigment composition, detritus proportion, backscattering coefficient, and so on. However, it is clearly seen that as CHLA changes, the absorption controls the reflectance in blue bands centered at 412, 443 and 490 nm while the scattering plays important role in determining the reflectance in 565 nm and 666 nm.

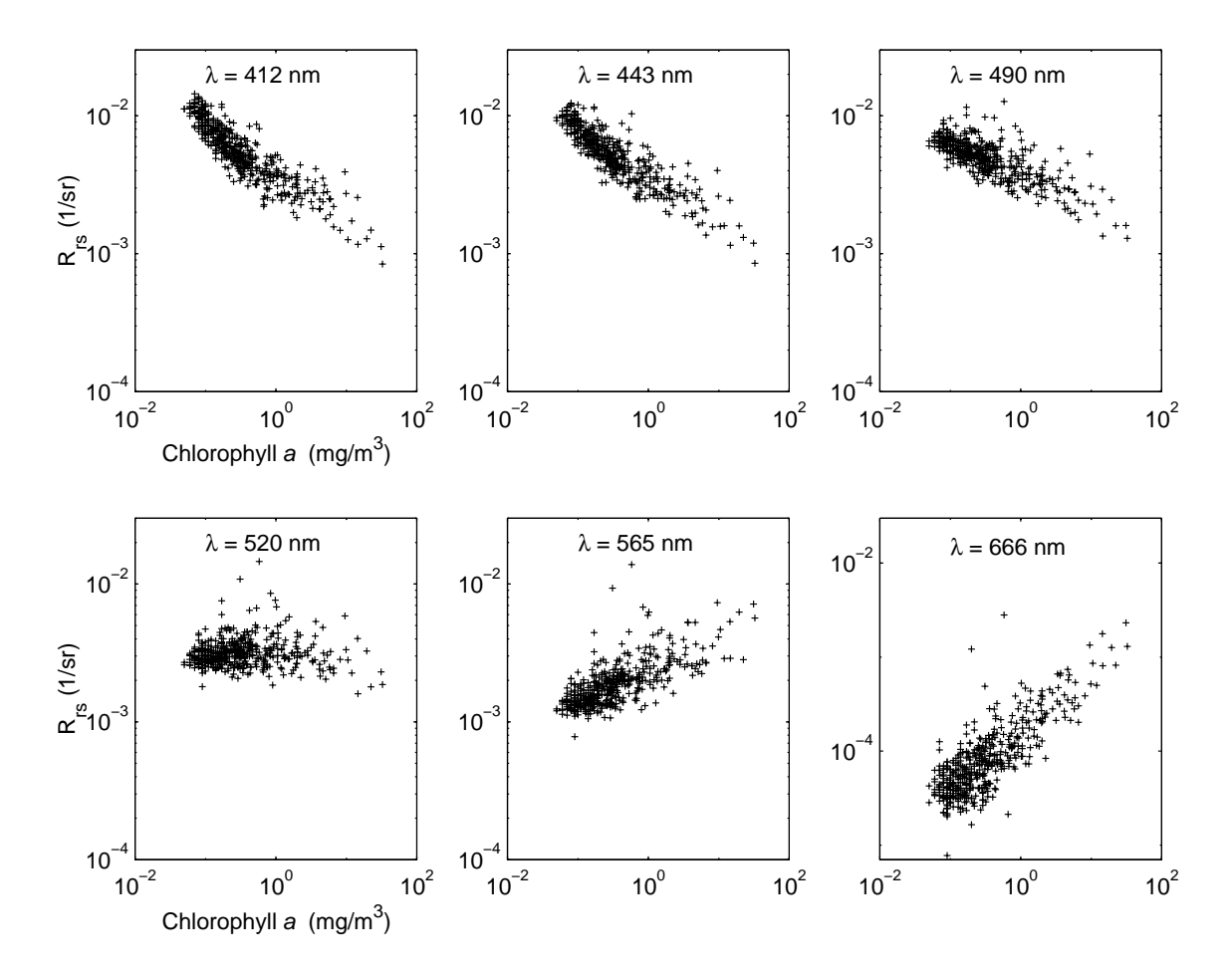


Figure 2. Chlorophyll a concentration and remote-sensing reflectance at six visible GLI channels from CalCOFI data set. The R_{rs} values have been estimated from underwater radiance/irradiance data. The data at 520- and 565-band were obtained by interpolation from the data of existing bands.

From these data, we derive the parameterization of particle absorption as a function of CHLA. The schematic of the whole procedure is shown in Figure 3. In first two steps shown in the figure, we estimated the particle backscattering coefficients

108 Proc. SPIE Vol. 4154

for individual data set. Then we obtain the total absorption and by subtracting the pure water absorption and CDOM absorption, we estimate the absorption coefficient of suspended particles.

First, we are to retrieve the absorption coefficient from $R_{rs}(\lambda)$ and CHLA. To do this, we need to know or assume the backscattering coefficient. Since current data set does not include backscattering coefficients, we had to estimate them by using an empirical model such as described in Morel¹³ or Carder, et al.⁴ The former model gives particle backscattering coefficient as a function of CHLA while the latter as a function of R_{rs} at some wavebands. The latter algorithm might describe well the local variability of b_{bp} that is not correlated to CHLA. However it was not used in this study since its wavebands are not matched to ours. The former model is well recognized as a good approximation for case 1 waters. However in local scale, the particle backscattering, b_{bp} is not so much correlated to phytoplankton or CHLA. It, in principle, results from the fact that the backscattering is largely determined by the presence of small particles rather than phytoplankton, while the contribution of phytoplankton to total backscattering is much smaller in most cases. It has been confirmed by previous extensive measurements^{6,19} and theoretical calculations. So if we directly apply Morel's backscattering model to estimate the absorption by particles and CDOM, apg, the estimated values are likely to have much variation around the true value and be negative when the absorption is small. As a result, the regression may not be made nicely. However, assuming that Morel's model is good approximation also for CalCOFI data set at least in average sense, we can use this model for initial estimation of the absorption by particle and CDOM, $a_{pg}(\lambda)$ for each data set. Even if these values of a_{pg} include error due to the difference between assumed and true backscattering coefficient for each station, we can get initial parameterization for apg by a simple quality control step and regression. This is STEP 1 in Figure 3. We include the quality control step because negative values are unrealistic and cannot be used for regression with power function. We divide the whole data into subgroups according to CHLA. For each subgroup, negative values and the same number of highest values removed simultaneously. This step is required because a significant number of app for 520- and 565-band shows negative value in low CHLA. In low CHLA stations, the value of app is small for these bands, so the noise in R_{rs} easily make the retrieved total absorption less than that due to pure water only. All regression for a_{pg} or a_p in this study were made in log-log space and with polynomials of up to third order, depending on the correlation coefficient.

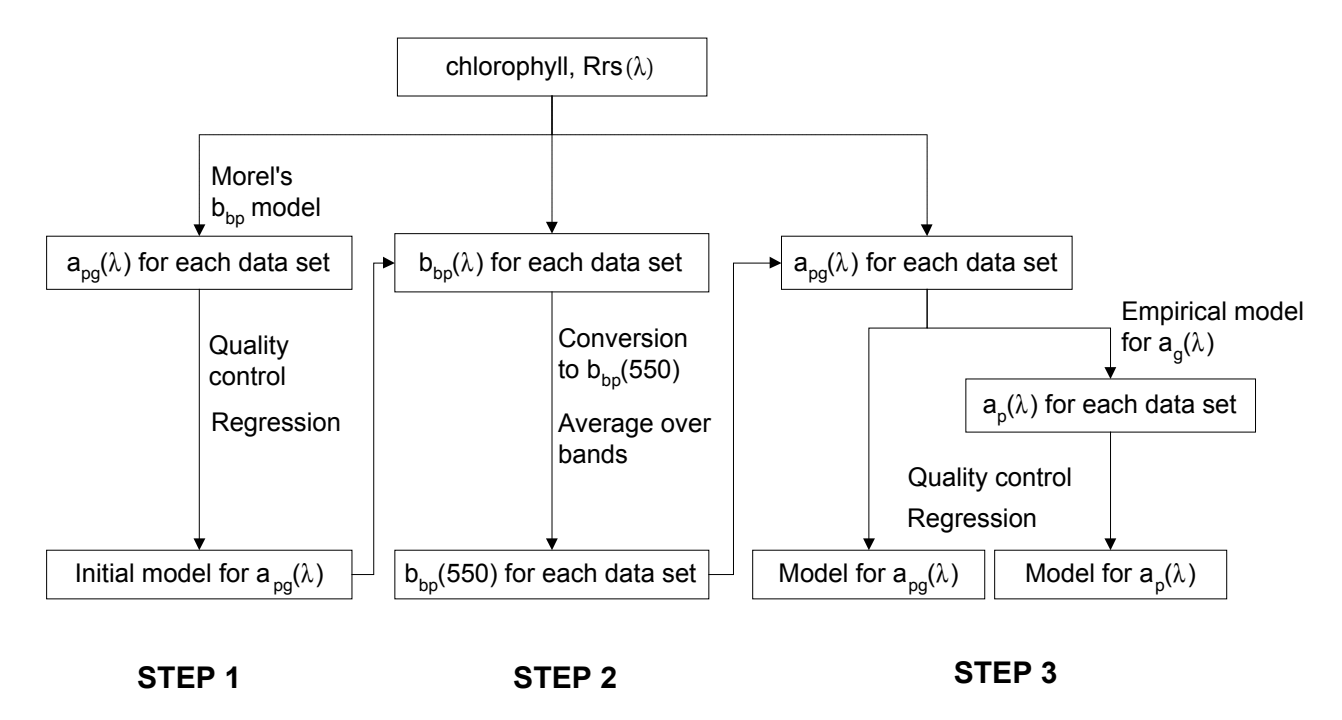


Figure 3. Procedure for estimation of the particle absorption coefficients from the data of chlorophyll and R_{rs}.

The second step, STEP 2 in Figure 3 is the procedure to estimate $b_{bp}(550)$ for each data set. Once we have the $a_{pg}(\lambda)$ as a function of CHLA, we can retrieve total backscattering coefficient. Then by subtracting the pure water component equal to half of $b_w(\lambda)$, its particle portion, $b_{bp}(\lambda)$ is obtained. These values of $b_{bp}(\lambda)$ from five bands can be converted to reference wavelength (550 nm) by applying the spectral behavior of particle backscattering. The spectral dependence of particle

backscattering can be expressed as λ^{-n} , where the exponent n is normally taken to be 1. In this study we also assume the value of 1 for n. Note actually varies 0 to 4, depending on the size distribution and refractive indices of scatterers. Now the obtained $b_{bp}(550)$ is fully accounted for the variability that does not covary with CHLA. The plot of $b_{bp}(550)$ is shown in bottom right side of Figure 4. Note it fully spans the limits of case 1 water, which denoted by dashed line.

Through STEP 3, we derive the models for absorption by suspended particles and CDOM, $a_{pg}(\lambda)$ and absorption by suspended particles, $a_p(\lambda)$. Using the $b_{bp}(550)$ averaged from five bands, we can easily compute $a_{pg}(\lambda)$ for each data set with radiance model. After the same quality-control step as in STEP 1 is done if necessary, regression gives the parameterization for $a_{pg}(\lambda)$ as a function of CHLA. The regression results are shown in Table 2. The numbers in parenthesis in second row mean chlorophyll specific absorption coefficient at 1mg/m^3 of CHLA. We also denote root-mean-square error (RMS Error), r-squared value (R-squared) and the number of data (N) that are used for fitting. Curve fitting was done using Eq. (4) with third order polynomials in log-transformed data when the curvature was apparent (not shown here but trend is similar as in Figure 4 (a) to (e)).

$$\log_{10} a_{pg}(\lambda) = \sum_{i=0}^{3} c(\lambda, i) [\log_{10} CHLA]^{i}, \qquad (4)$$

where coefficients $c(\lambda,i)$ are determined by regression.

The curvature may result from the assumed model for particle backscattering coefficient as a function of CHLA. This remains to be checked by *in situ* measurements of IOP in future. We used a quadratic and a linear equation for 520-, and 565-bands, respectively in log-log space because higher order feature is not apparent. In regression of $a_{pg}(520)$ and $a_{pg}(565)$, the numbers of data were reduced by quality control. The estimated values of a_{pg} are highly correlated to measured CHLA except 565 nm-band. This model is very useful for retrieval of CHLA when a_{g} is considered to be negligible or correlated to CHLA as generally assumed in case 1 waters.

Table 2. The parameterization of absorption by particles and CDOM, $a_{pg}(\lambda)$, using Eq. (4). RMS error and R-squared are computed in normal space, not in log-log space.

wavelength (nm)	412	443	490	520	565
c(λ,0)	-0.945 (0.114)	-1.034 (0.092)	-1.241 (0.0575)	-1.471 (0.0338)	-1.698 (0.020)
c(λ,1)	0.556	0.615	0.682	0.787	0.347
c(λ,2)	-0.080	-0.080	-0.105	-0.099	0.0
c(λ,3)	0.067	0.043	0.024	0.0	0.0
RMS error	0.020	0.010	0.0051	0.0061	0.0125
R-squared	0.96	0.98	0.99	0.98	0.37
N	459	459	459	435	371

In general, the absorption by CDOM does not seem correlated to CHLA even in case 1 waters. So it is useful to assess the contribution of CDOM to total absorption from remotely measured ocean-color data. For this purpose, we need to separate $a_p(\lambda)$ and $a_g(\lambda)$ from $a_{pg}(\lambda)$. We use empirical algorithm for $a_g(440)$ developed for ADEOS-II/GLI standard product generation. Previous studies have confirmed CDOM absorption decrease exponentially with wavelength from near-UV to visible domain: $a_g(\lambda)=a_g(\lambda_0)\exp(-S(\lambda-\lambda_0))$. The spectral constant, S is relatively stable parameter, ranging 0.010 to 0.020, which is dependent on chemical composition of dissolved organic matter. In oceanic waters, the constant S varies in more restricted range around the average value that may be dependent on area. Therefore, we take 0.0185 for the constant, S in this study. This value is average of a number of measurements in California Current. With this spectral behavior, absorption by CDOM in other wavebands can be estimated. With the estimation of $a_g(\lambda)$, $a_p(\lambda)$ was separated from $a_{pg}(\lambda)$. Finally, after quality control for data of $a_p(520)$ and $a_p(565)$, regression was performed as a function of CHLA. The regression results using Eq. (5) are shown in Table 2. We also show the chlorophyll specific values at 1mg/m^3 of CHLA in parenthesis, RMS error, R-squared and the number of data.

$$\log_{10} a_{p}(\lambda) = \sum_{i=0}^{3} d(\lambda, i) [\log_{10} CHLA]^{i},$$
(5)

where coefficients, $d(\lambda, i)$ are determined by regression.

Table 3. The parameteriztion of absorption by particles, $a_p(\lambda)$, using Eq. (5). RMS error and R-squared are computed in normal space, not in log-log space.

wavelength (nm)	412	443	490	520	565
$d(\lambda, 0)$	-1.206(0.0622)	-1.198(0.0634)	-1.341 (0.0456)	-1.568 (0.0270)	-1.727 (0.0188)
d(λ, 1)	0.650	0.679	0.710	0.835	0.322
$d(\lambda, 2)$	-0.024	-0.050	-0.103	-0.077	0.0
$d(\lambda, 3)$	0.059	0.045	0.052	0.0	0.0
RMS error	0.0134	0.0055	0.0043	0.0073	0.0125
R-squared	0.97	0.99	0.99	0.97	0.33
N	459	459	459	408	355

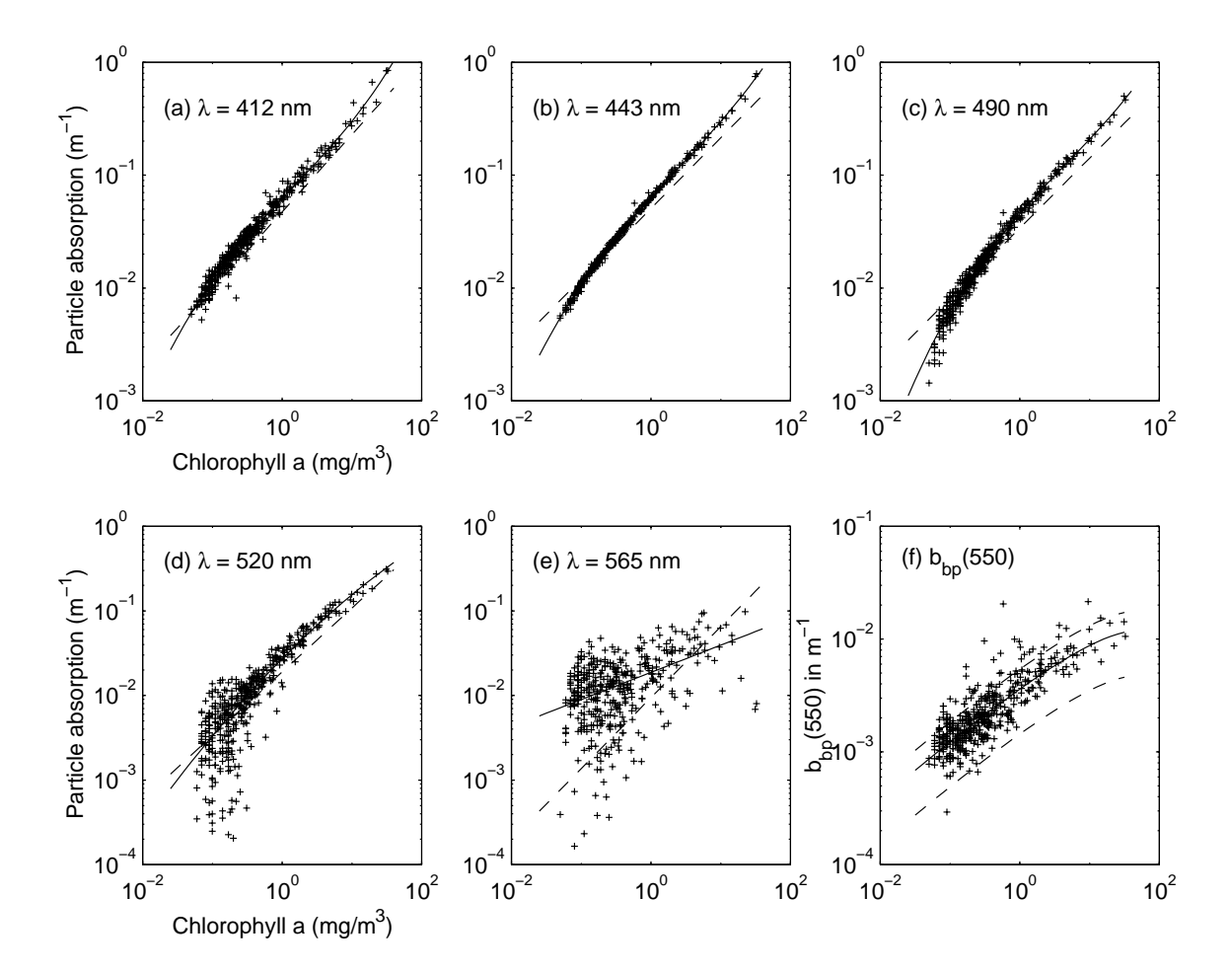


Figure 4. Particle absorption coefficients at 412, 443, 490, 520 and 565 nm ((a) to (e)) and particle backscattering coefficients at 550 nm ((f)). Solid lines denote fitted curves whose parameters are in Table 2 and dashed lines denote the models of Bricaud et al., 1998 ((a) to (e)). Morel's model for particle backscattering coefficients in case 1 waters is also plotted with dashed lines for upper and lower limits ((f)).

Figure 4 shows the data of $a_p(\lambda)$ with best fitted line (solid line). We can see quite low scatter in a_p values for a given CHLA at 412, 443, and 490 nm. This is a combined effect of (1) signal to noise of R_{rs} is high for low a_p values in these bands, (2) background absorption by water is small, and (3) the correlated variance in R_{rs} values for same value of CHLA can be effectively removed by correction of station-dependent particle backscattering coefficients. The dashed lines in Figure 4(a)-

(e) shows the models of Bricaud et al., 19989 that were derived by statistical analysis for extensive measurements. The two models are almost consistent in blue bands, taking into consideration for confidence range described in that paper. For CHLA range of 0.1 to 0.5 mg/m³, both models show very good agreement. However, we can see systematic differences between the two. The slopes of $a_0(443)$ and $a_0(490)$ with increasing CHLA are higher in this study. Despite these difference is small compared to regional variability of particle absorption pointed out in other studies, 22-24 these can cause significant errors in retrieval of CHLA, a_g(440) and b_{bp}(550) when they are to be retrieved simultaneously. For 565 nm band, the model derived from R_{rs} show comparatively large uncertainties. Fortunately, at this wavelength, water absorption usually exceeds particle absorption and the difference in total absorption is much smaller for low and moderate CHLA. However, the difference can make significant effect in retrieval for high CHLA.

4. APPLICATION TO INVERSION ALGORITHM

In section 3, we derived a model for particle absorption coefficients from in situ data of R_{rs} and CHLA, aiming at application to retrieval of CHLA, CDOM absorption at 440 nm(ag(440)), and particle backscattering coefficient at 550 nm (b_{bp}(550)). So it is important to test the derived model by applying it to an inversion algorithm. We used the radiance model and IOP models same as those used for derivation of the particle absorption model, which are described section 2. In Figure 5, we show the retrieved results of CHLA, $a_g(440)$, and $b_{bo}(550)$, which are compared with the desired ones. Note that the desired values for CHLA are in situ CHLA. On the other hand, for a_g(440) and b_{bp}(550), the desired values are the assumed values for derivation of the model of particle absorption coefficient. In other words, desired values for $a_g(440)$ are given by the empirical algorithm of Mitchell²⁰ and the desired values for $b_{bp}(550)$ are shown in Figure 4 (panel (f)). We can see that CHLA and b_{bp}(550) can be retrieved with relatively good accuracy, but a_g(440) retrieval shows much diverse than the desired value and often negative. The reason for this is that CDOM absorption is usually smaller than particulate absorption as in most oceanic waters. Therefore, to retrieve a_e(440) in such waters, accurately calibrated and high sensitivity for nLw is required as well as well-matched model of particle absorption.

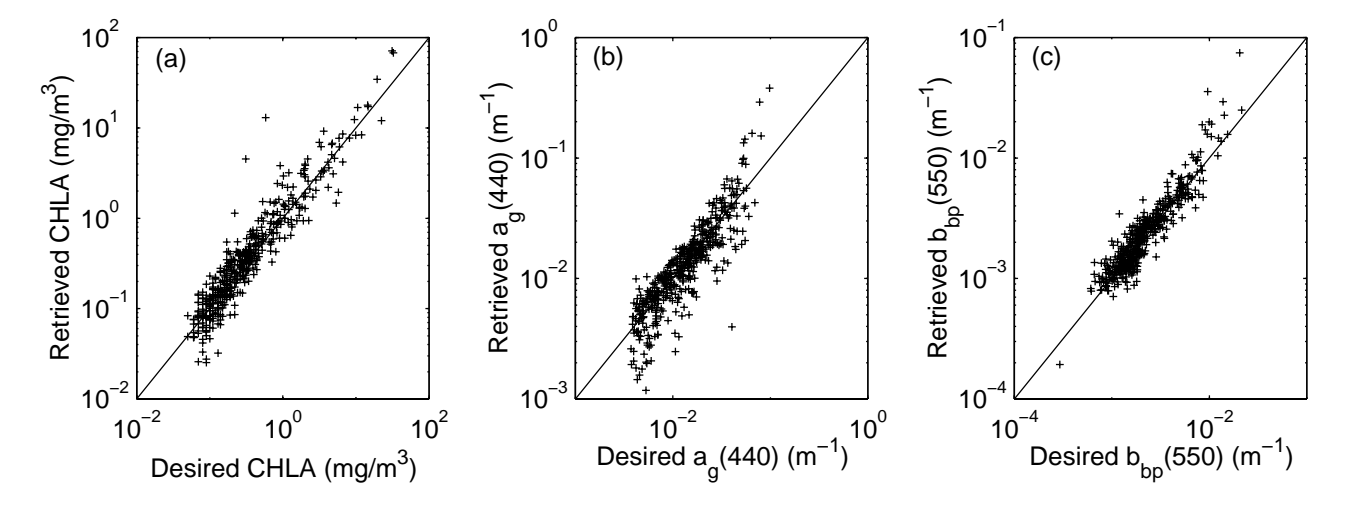


Figure 5. Application of the model of particle absorption to retrieve chlorophyll a concentration (a); CDOM absorption at 440 nm, (b); and particle backscattering coefficient at 550 nm, (c).

5. CONCLUSIONS

In conclusion, we have derived models for absorption by particles, $a_p(\lambda)$, and absorption by particles and CDOM, $a_{pg}(\lambda)$, at wavebands centered on 412, 443, 490, 520 and 565 nm as a function of CHLA, from CalCOFI data set (R_{rs} and CHLA). The retrieved absorption coefficients exhibit very low level of scatter around regression lines for a given CHLA except at 565 nm. The advantage of this approach is that the derived models of ap and apg are best fitted to the in situ reflectance data and reflectance model. It means these models should give better retrieval of CHLA when applied to inversion algorithm, compared to the models directly derived from *in situ* measurements of absorption coefficients.

We have demonstrated the retrieval of CHLA, $a_g(440)$ and $b_{bp}(550)$ by the inversion of R_{rs} data. The retrieved CHLA has good agreement with measured CHLA and the retrieval of $a_g(440)$ and $b_{bp}(550)$ has shown to be reasonable.

We have employed commonly-used several assumptions including the average coefficient of particle backscattering as a function of CHLA and its spectral dependence, and we have used an empirical algorithm for CDOM absorption and averaged slope constant. Recently, advance optical measurement techniques for measuring several IOPs are developed and more complete bio-optical measurement is feasible. The derived models can be improved in future if more complete sets of bio-optical parameters are available.

ACKNOWLEDGMENTS

We are very grateful to Curtis D. Mobley for allowing us to use Hydrolight code and Annick Bricaud for providing the model coefficients of particle absorption. We thank Hajime Fukushima for encouraging this study. This work was supported by ADEOS-II/GLI project.

REFERENCES

- 1. J.E. O'Reilly, S. Maritorena, B.G. Mitchell, D.A. Siegel, K.L. Carder, S.A. Garver, M. Kahru, and C. McClain, "Ocean color chlorophyll algorithms for SeaWiFS", *J. Geophys. Res.* 103, pp 24937-24953, 1998.
- 2. S.A. Garver and D.A. Siegel, "Inherent optical property inversion of ocean color spectra and its biogeochemical interpretation 1. Time series from the Sargasso Sea", *J. Geophys. Res. 102*, pp18607-18625, 1997.
- 3. F.E. Hoge and P.E. Lyon, "Satellite retrieval of inherent optical properties by linear matrix inversion of oceanic radiance models: An analysis of model and radiance measurement errors", *J. Geophys. Res.* 101, pp16631-16648, 1996.
- 4. K.L. Carder, F.R. Chen, Z.P. Lee, S.K. Hawes, and D. Kamykowski, "Semianalytic Moderate-Resolution Imaging Spectrometer algorithms for chlorophyll *a* and absorption with bio-optical domains based on nitrate-depletion temperatures", *J. Geophys. Res.* 104, pp5403-5421, 1999.
- 5. K.L. Carder, R.G. Steward, G.R. Harvey, and P.B. Ortner, Marine humic and fulvic acids: Their effects on remote sensing reflectance, *Limnol. Oceanogr.* 34, pp68-81, 1989.
- 6. H. Loisel and A. Morel, "Light scattering and chlorophyll concentration in case 1 waters: A reexamination", *Limnol. Oceanogr.* 43, pp 847-858, 1998.
- 7. H.R. Gordon, O.B. Brown, R.H.Evans, J.W. Brown, R.C.Smith, K.S. Baker, and D.K.Clark, "A semianalytical radiance model of ocean color", *J. Geophys. Res.* 93, pp 10909-10924, 1998.
- 8. A. Morel and A. Bricaud, "Theoretical results concerning light absorption in a discrete medium and application to the specific absorption of phytoplankton, *Deep Sea Res.*, *Part A*, *28*, pp1357-1393, 1981
- 9. A. Bricaud, A. Morel, M. Babin, K. Allali and H. Claustre, "Variations of light absorption by suspended particles with chlorophyll *a* concentration in oceanic (case 1) waters: analysis and implications for bio-optical models", *J. Geophys. Res.* 103, pp 31033-31044, 1998
- 10. A. Morel and B. Gentili, "Diffuse reflectance of oceanic waters, II, Bidirectional aspects", *Appl. Opt. 32*, pp 6864-6879, 1993.
- 11. Z.P. Lee, K.L. Carder, C.D. Mobley, R.G. Steward, and J.S. Patch, "Hyperspectral remote sensing for shallow waters: 1. A semianalytical model", *Appl. Opt. 37*, pp 6329-6338, 1998.
- 12. J.R. Zaneveld, "A theoretical derivation of the dependence of the remotely sensed reflectance of the ocean on the inherent optical properties", *J. Geophys. Res.* 100, pp 13135-13142, 1995.
- 13. A. Morel, "Optical modeling of the upper ocean in relation to its biogenous matter content (case I waters)", *J. Geophys. Res.* 93, pp 10749-10768, 1988.
- 14. C.D. Mobley, Light and Water: Radiative Transfer in Natural Waters, Academic, New York, 1994.
- 15. C.D. Mobley, Hydrolight 3.0 Users' Guide, Final Report, SRI International, Menlo Park, California, 1995.
- 16. R.M. Pope and E.S. Fry, "Absorption spectrum (380-700 nm) of pure water. II. Integrating cavity measurements", *Appl. Opt. 36*, pp 8710-8723, 1997.
- 17. R. Smith and K.S. Baker, "Optical properties of the clearest natural waters (200-800 nm)", *Appl. Opt. 20*, pp 177-184, 1981
- 18. B.G. Mitchell and M. Kahru, "Algorithms for SeaWiFS standard products developed with the CalCOFI bio-optical data set", *CalCOFI Rep., Vol.* 39, pp 133-147, 1998.
- 19. J.C. Kitchen and J.R.V. Zaneveld, "On the noncorrelation of the vertical structure of light scattering and chlorophyll a in case I waters", *J. Geophys. Res.* 95, pp 20237-20246, 1990.

- 20. B.G. Mitchell, *ADEOS-II/GLI Documents: Algorithm Description*, ver 1.0, Chapter 3.2.2, National Space Development Agency of Japan, 1999.
- 21. A. Bricaud, A. Morel, and L. Prieur, "Absorption by dissolved organic matter of the sea (yellow substance) in the UV and visible domains", *Limnol. Oceanogr.* 26, pp 43-53, 1981.
- 22. B.G. Mitchell, "Predictive bio-optical relationships for polar oceans and marginal ice zones", *J. Mar. Sys. 3*, pp91-105, 1992.
- 23. B.G. Mitchell and O. Holm-Hansen, "Bio-optical properties of Antarctic Peninsula waters: differentiation from temperate ocean models", *Deep-Sea Res. 38*, pp 1009-1028, 1991.
- 24. T. Hirawake, H. Satoh, T. Ishimaru, Y. Yamaguch and M. Kishino, "Bio-optical relationship of Case 1 waters: The difference between the low- and mid-latitude waters and the Southern Ocean", *J.Oceanogr.* 56, pp245-260, 2000.

ABBREVIATIONS AND SYMBOLS

IOP AOP	inherent optical property apparent optical property
CHLA	chlorophyll a concentration
CDOM	colored dissolved organic matter
$R_{rs}(\lambda)$	remote sensing reflectance at wavelength λ
$r_{rs}(\lambda)$	ratio of upwelling radiance to downward irradiance just below the surface at wavelength $\boldsymbol{\lambda}$
$nLw(\lambda)$	normalized water-leaving radiance at wavelength λ
$a(\lambda)$	total absorption coefficient at wavelength λ
$a_{\rm w}(\lambda)$	absorption coefficient of pure water at wavelength λ
$a_g(\lambda)$	absorption coefficient of CDOM or <i>gelbstoff</i> at wavelength λ
$a_p(\lambda)$	absorption coefficient of suspended particles at wavelength λ
$a_{pg}(\lambda)$	sum of $a_p(\lambda)$ and $a_g(\lambda)$
$b(\lambda)$	total backscattering coefficient at wavelength λ
$b_{bw}(\lambda)$	backscattering coefficient of pure water at wavelength λ
$b_{bp}(\lambda)$	backscattering coefficient of suspended particles at wavelength λ
$L_u(0-,\lambda)$	upwelling radiance just below the surface at wavelength λ
$E_d(0-,\lambda)$	downward irradiance just below the surface at wavelength λ

114 Proc. SPIE Vol. 4154